# A bending wave simulator for investigating directional vibration sensing in insects

Ronald N. Miles,[a] Reginald B. Cocroft,[b] Colum Gibbons, and Daniel Batt
*Department of Mechanical Engineering, State University of New York, Binghamton, New York 13902*

(Received 12 September 2000; revised 2 March 2001; accepted 7 March 2001)

Substrate vibrations are important in social and ecological interactions for many insects and other arthropods. Localization cues include time and amplitude differences among an array of vibration detectors. However, for small species these cues are greatly reduced, and localization mechanisms remain unclear. Here we describe a method of simulating the vibrational environment that facilitates investigation of localization mechanisms in small species. Our model species was the treehopper *Umbonia crassicornis* (Membracidae; length 1 cm), which communicates using bending waves that propagate along plant stems. We designed a simulator consisting of a length of dowel and two actuators. The actuators were driven with two time signals that created the relationship between slope and displacement characteristic of steady-state bending wave motion. Because the surface of the dowel does not bend, as would a natural stem, close approximation of bending wave motion was limited to a region in the center of the dowel. An example of measurements of the dynamic response of an insect on the simulator is provided to illustrate its utility in the study of directional vibration sensing in insects. © *2001 Acoustical Society of America.* [DOI: 10.1121/1.1369106]

PACS numbers: 43.80.Ev, 43.80.Gx, 43.40.Yq, 43.40.At [WA]

## I. INTRODUCTION

Substrate-borne vibrations are important in social and ecological interactions for many insects and other arthropods (reviewed in Markl, 1983; Gogala, 1985; Henry, 1994; Stewart, 1997; Barth, 1998). In contexts such as mate searching or prey detection, it is often necessary to locate the vibration source. In principle, the direction of propagation of substrate vibrations can be determined using differences in arrival time or amplitude between detectors that are sufficiently widely spaced. Vibration receptors in arthropods are typically in the legs (e.g., Kalmring, 1985), which form an array of detectors in contact with the substrate. For relatively large species (with legs spanning 5 to 10 cm), individuals are able to determine source direction using either arrival time differences (Brownell and Farley, 1979; Hergenroder and Barth, 1983; Aicher and Tautz, 1990) or an amplitude gradient (Brownell and Farley, 1979; Latimer and Schatral, 1983; Hergenroder and Barth, 1983; Cokl *et al.*, 1985). However, the size range of species using substrate vibration spans over two orders of magnitude. Smaller species are faced with a more difficult localization task. Stimulus wavelengths are many times longer than the insects' dimensions, and the time and amplitude differences among inputs are extremely small. It is not clear that the mechanisms used by large species can function at these smaller scales (see Brownell, 1977; Cokl *et al.*, 1985). If not, then any localization by small species must employ as-yet unknown directional mechanisms.

The scaling problem encountered in locating a vibration source is paralleled in acoustic sensing. For airborne sound, however, there is a clearer understanding of the mechanisms used at different size scales. The solutions provided by very small species in locating a sound source might therefore suggest mechanisms that can be applied across modalities. In sound localization, very small species can use a form of mechanical pre-processing to enhance directional cues. This principle is illustrated by the fly *Ormia ochracea* (Tachinidae), which locates singing crickets using sound wavelengths over 200 times greater than the distance between its two tympanal hearing organs. The biomechanical response of the tympana, which are mechanically coupled, converts an interaural time difference of 1.5 microseconds into large, directional amplitude differences that can be easily detected by the nervous system (Miles *et al.*, 1995).

In general, the form of mechanical directionality seen in the fly ear can be produced by the interaction of two resonant modes of vibration in a structure that responds to propagating waves (Miles *et al.*, 1995). One mode must respond to the phase, or the spatial gradient of the quantity being detected, while the other mode must respond to the spatial average of the quantity over the region sampled. Given these response properties, the two modes can combine to convert a small phase difference across the region into a large amplitude difference at different points on the structure (Gerzon, 1994). An analogous form of mechanical directionality could in principle be produced by a system responding to vibrational waves propagating across a substrate. In insects, however, the design of the system is likely to differ substantially from those used in sound reception. While sound receptors in insects are located within specialized exoskeletal structures that respond to pressure waves, vibration receptors are located in more generalized structures such as the legs. Mechanical directionality in the response to substrate vibrations, if it exists, is thus likely to involve motion of the body as a whole rather than of a localized sensory structure. If the primary receptors are in the legs, these are likely to respond to relative motion between the body and the substrate. Detect-

[a]Electronic mail: miles@binghamton.edu
[b]Present address: Division of Biological Sciences, University of Missouri, Columbia, MO 65211.

ing the propagation direction of waves on the substrate would then involve processing differences in the responses of receptors on different legs.

The properties of natural vibrational environments pose challenges for investigating the influence of direction on an insect's mechanical response to substrate vibration. Foremost is the heterogeneity and severe filtering properties of natural substrates (Michelsen *et al.*, 1982; Keuper and Kuhne, 1983). Because of these unpredictable influences on vibration transmission, it is difficult to deliver stimuli that are identical in every respect but propagation direction. For example, using a natural substrate, with two drivers some distance apart and an insect in the middle, the substrate will introduce changes in stimulus phase and frequency spectrum that can be difficult to compensate for. For these reasons, a careful investigation of mechanical directionality requires greater control over the vibrational environment experienced by the insect.

In this report we describe a new method for investigating the role of direction in the mechanical response to substrate vibrations, one that provides precise control over the vibrational environment. Our study system is a small insect that communicates using bending waves traveling through the stems of plants. We designed a simulator that provides accurate control of the frequency, intensity, and direction of propagation of a vibration stimulus. We first describe the study species and its natural vibrational environment. We then present the theoretical background used to simulate this environment. Finally, we describe the performance of the simulator relative to ideal bending waves propagating along a stem. We also illustrate the use of the simulator with an example of data that suggest directionality in the dynamic response of an insect to substrate vibrations.

## II. STUDY SYSTEM

The stems and leaves of plants constitute one of the most widespread substrates used by arthropods in communication and predator-prey interactions (Henry, 1994; Stewart, 1997). In theory, a number of wave types could propagate along a rodlike structure such as a plant stem (Markl, 1983; Gogala, 1985; Cremer and Heckl, 1988). However, the most important wave type for biological interactions is bending waves (Cocroft *et al.*, 2000 and references therein). Because of the potential in natural substrates for reflected waves and unpredictable amplitude attenuation patterns, vibration transmission in nature will not always resemble a pure bending wave propagating in one direction along an ideal beam (e.g., Michelsen *et al.*, 1982). However, in spite of these constraints, bending waves are known to be used by insects and spiders that communicate using plant-borne vibrations (Michelsen *et al.*, 1982; Keuper and Kuhne, 1983; Barth, 1993, 1998).

The thornbug treehopper *Umbonia crassicornis* (Membracidae) is a sap-feeding insect about 1 cm long. Thornbugs spend most of their lives on the surface of their hostplants, and for much of this time they are sedentary (Wood, 1983). Accordingly, all of our vibration measurements have been made using freestanding individuals. The ability to do this is important, because restraining the insects would alter the mechanical response of the body. This species is also an appropriate study system because substrate-borne vibrations are central to their biology. Both adults and juveniles use communication signals that propagate through the plant in the form of bending waves (Cocroft *et al.*, 2000). These signals function in parent-offspring interactions (Cocroft, 1996, 1999) and in the mate-locating behavior of adults (Cocroft personal observations). Most of the energy in these signals is below 4000 Hz (Cocroft, 1999).

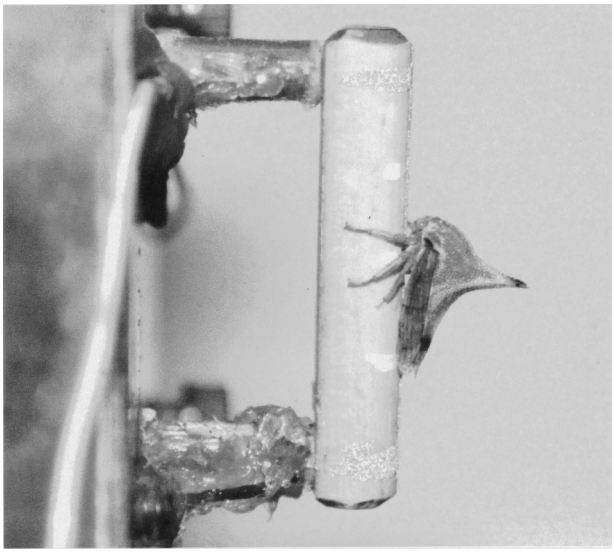

FIG. 1. *Umbonia crassicornis* (total length 10 mm) on the bending wave simulator. The insect's feet occupy a portion of the dowel (length 30 mm, diameter 6 mm) extending less than 1/8th the distance between the actuators in either direction from the middle. It is necessary to simulate a bending wave only over this narrow portion. From Cocroft *et al.* (2000), reprinted with permission.

## III. THEORY

Our goal was to create a simulator that produced a vibration environment at the insect's feet that closely resembled that due to steady-state bending wave motion. We then wished to examine the mechanical response of the insect's body to the direction of substrate vibration; i.e., how the body moves relative to the substrate when the stimulus propagates from in front of or behind the insect. To measure the influence of direction on the mechanical response of the body, we needed to be able to electronically switch the direction of propagation between measurements, without altering the position or posture of the insect.

The simulator, as shown in Fig. 1, consists of a short segment of dowel (30 mm long, 6 mm in diameter) with piezoceramic actuators on each end. The actuators were bonded to the dowel with epoxy parallel to each other and perpendicular to the long axis of the dowel. The other ends of the actuators were bonded to a rigid metal fixture. Signals input into the actuators created motions at each end of the dowel so that the motion at its center mimicked that of bending waves on a typical host plant stem. The diameter of the dowel is similar to that of typical host plant stems, and the insect rests on the stem in a natural position.

In order to simulate bending wave motion at the center of the dowel, the two actuators must create a carefully con-

trolled combination of displacement and slope at the center. To examine the type of motion the simulator needs to create, consider the equation of motion for a beam in bending,

$$EI\frac{\partial^4 w(x,t)}{\partial x^4}+\rho A\ddot{w}(x,t)=0, \tag{1}$$

where $E$ is Young's modulus of elasticity, $I$ is the area moment if inertia, $w(x,t)$ is the beam displacement, $\rho$ is the mass density, and $A$ is the cross sectional area. $x$ is the position along the beam and $t$ is time.

If we assume that a steady-state bending wave travels in the positive direction the response can be written as

$$w(x,t)=We^{\hat{\imath}(\omega t-kx)}, \tag{2}$$

where $W$ is the amplitude, $\omega$ is the frequency in radians/second, $\hat{\imath}=\sqrt{-1}$, $k=\omega/c$ is the wave number, and $c$ is the propagation speed of the wave. Substitution of Eq. (2) into Eq. (1) gives the phase speed,

$$c=\sqrt{\omega}\left(\frac{B}{\rho A}\right)^{1/4}. \tag{3}$$

The propagation velocity of bending waves will vary in relation to the characteristics of the particular stem through which they are traveling. This velocity can be expressed as

$$c\approx c_c\sqrt{f}, \tag{4}$$

where $c_c$ is a constant and $f$ is the frequency in hertz. Measurements of the phase propagation velocity of bending waves in plant systems yield estimates of $c_c$ ranging from 1.3 to 2.5 (calculated from data in Michelsen *et al.*, 1982). Phase propagation velocities measured in stems of *U. crassicornis* host plants (*Calliandra haematocephala*) yield estimates of $c_c$ of 2.2 and 2.4 (Cocroft, unpublished data). For this study we chose a value of 2.4 (this value can easily be changed if a different velocity is desired). The wave number may then be expressed as

$$k=\frac{\omega}{c}=\frac{2\pi f}{c_c\sqrt{f}}=2\pi\sqrt{f}/c_c, \tag{5}$$

with units of radians/meter.

Because the simulator consists of a rigid dowel supported on two actuators (Fig. 1) it is possible to control only the slope and displacement of the motion at a given point along its length. The rigidity of the dowel does not allow actual bending motion which requires curvature of the substrate. This somewhat simplified apparatus does, however, permit us to closely approximate the displacement and rotation due to true bending wave motion, at least for a region at the center of the dowel. To do this, we need to determine the required motion at each end of the dowel such that the middle of the dowel has the desired relationship between slope and displacement.

For a displacement given by Eq. (2), the slope of the substrate is

$$w_x(x,t)=-\hat{\imath}kWe^{\hat{\imath}(\omega t-kx)}. \tag{6}$$

From Eqs. (2) and (6) it can be seen that the transfer function between the displacement and slope at any point will be

$$H_{ww_x}(\omega)=-\hat{\imath}k. \tag{7}$$

Our goal is to impose motion at the ends of the dowel such that the response in the vicinity of the insect follows Eq. (7). Let the displacements imposed at the ends of the dowel be $y_1(t)$ and $y_2(t)$. If we assume that the dowel remains rigid, the displacement, $y_m(t)$, and the slope, $\theta_m(t)$ at the middle will be

$$y_m(t)=\frac{y_1(t)+y_2(t)}{2},\quad \theta_m(t)=\frac{y_2(t)-y_1(t)}{d}, \tag{8}$$

where $d$ is the length of the dowel. Equations (8) enable us to relate the transfer function between the motions at the ends of the dowel, $H_{y_1y_2}(\omega)$, to transfer function between the displacement and slope at the middle, $H_{y_m\theta_m}(\omega)$,

$$H_{y_1y_2}(\omega)=\frac{1+(d/2)H_{y_m\theta_m}(\omega)}{1-(d/2)H_{y_m\theta_m}(\omega)}=\frac{1-\hat{\imath}kd/2}{1+\hat{\imath}kd/2}, \tag{9}$$

where we have assumed that the relationship between displacement and slope at the middle of the dowel should be the same as given in Eq. (7),

$$H_{ww_x}(\omega)=-\hat{\imath}k=H_{y_m\theta_m}(\omega). \tag{10}$$

If it is possible to create two random displacements at the ends of the dowel, $y_1(t)$ and $y_2(t)$ that are related to each other through the transfer function given in Eq. (9), then the motion at the middle of the dowel will provide a reasonable simulation of a traveling bending wave.

Of course, since the dowel is assumed to remain straight, it clearly will not accurately represent bending motion over its entire length. If one wishes to design a simulator for bending waves over a specified range of frequencies and over a known portion of the dowel, it is helpful to be able to estimate the expected discrepancy between the motion of the dowel at each location along its length and the desired bending wave motion. Given the displacement and slope at the middle of the dowel, $y_m(t)$ and $\theta_m(t)$, the displacement at any point is given by

$$y(x,t)=y_m(t)+x\theta_m(t), \tag{11}$$

where $x$ denotes the position along the dowel relative to the middle point. By using Eq. (11) it can be shown that the transfer function, $H_{y\theta_m}(\omega)$, between the displacement at any point, $y(x,t)$, and the slope $\theta_m(t)$, is

$$H_{y\theta_m}(\omega)=\frac{H_{y_m\theta_m}(\omega)}{(1-\hat{\imath}kx)}. \tag{12}$$

The ratio of the simulated and desired transfer functions as a function of position along the dowel is then

$$\frac{H_{y\theta_m}(\omega)}{H_{y_m\theta_m}(\omega)}=\frac{1}{(1-\hat{\imath}kx)}. \tag{13}$$

Equation (13) may be used to determine the error in the bending wave simulation as a function of position. The value of $k$ may be determined as in the discussion preceding Eq. (5).

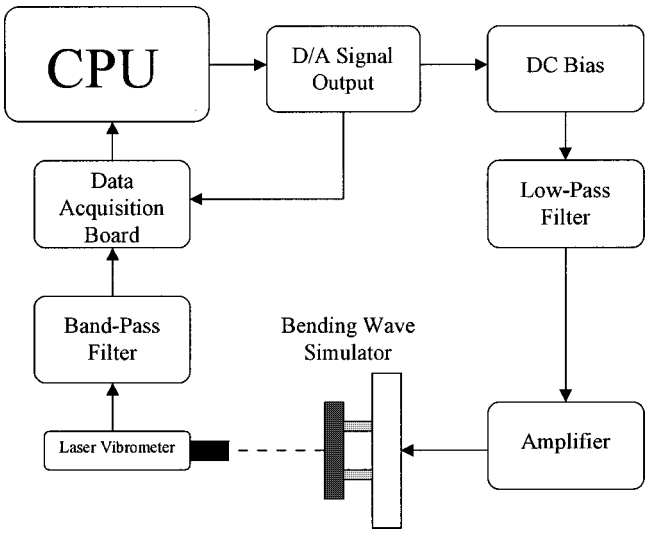


FIG. 2. Experimental setup for the bending wave simulator.

## IV. METHODS

### A. Experimental setup

A schematic of the experimental setup is shown in Fig. 2. A personal computer was used to generate the random signals sent to the actuators on the dowel and to acquire and analyze the vibration data. Random signals were used because they are very convenient for characterizing the dynamic response, which was the primary interest in this study. If the simulator is to be used for behavioral studies, the system will be modified to simulate insect calls. A Microstar DAP 2400/6 data acquisition PC board was used to output the two analog signals to drive the actuators. These two signals had the relative phase and amplitude needed to simulate bending wave motion in the central portion of the dowel. The details of the two-channel signal generation algorithm are given in the appendix. In order to drive the actuators, it was necessary to add a DC bias to the signals. The analog outputs of the DAP were low-pass filtered at 6 kHz by a Frequency Devices 90002 filter (48 dB/octave) and amplified by a DC coupled, Techron 5515 power amplifier before being sent to the pair of electrostrictive actuators (Xinetics XIRP0410L).

Motion of the simulator was measured with laser vibrometry, using a Polytec OFV 3000 controller and OFV 302 sensor head. The laser was positioned about 20 cm from the dowel, in the plane of motion of the actuators. The laser output was high-pass filtered at 100 Hz and low-pass filtered at 6 kHz using a Krohn–Hite 3550 filter (24 dB/octave). This signal, along with the two (AC coupled) output signals, was acquired using an Analogic FAST16 data acquisition board.

A compensation procedure was first run to account for differences in the output of the two actuators or in the amplitude of the two channels of the power amplifier. Identical signals were sent to the two actuators; the dowel motion produced at the site of each actuator was measured (with the other actuator silent) to obtain a calibration transfer function. This transfer function was used to correct the signal input into the lower of the two actuators so that it responded with the same amplitude and phase as the upper actuator. Absolute amplitude of the actuator output was adjusted to be similar to that of the insects' communication signals. As reported by Cocroft *et al.* (2000), RMS values from measurements of signals created by insects on typical plant stems ranged from 0.2 mm/s for females to 1.3 mm/s for males. RMS values for simulated random noise signals on the dowel near the insect's tarsus ranged from 0.1 mm/s to 0.3 mm/s.

Each measurement was stored in the form of a transfer function relative to the random signal sent to the upper actuator (acquired by the FAST16 board). Using the output signal as a standard allowed us to then compare nonsimultaneous measurements made along the dowel and thus characterize motion of the dowel as a whole.

The laser vibrometer and the simulator were mounted on a Newport RS 6000 $3'\times6'\times8''$ Optical Table to ensure that environmental vibrations did not influence the measurements.

### B. Simulator performance

To examine the accuracy of the simulated bending waves, response measurements were made at nine equally spaced points along the entire length of the dowel. As mentioned above, all data were stored as transfer functions between the displacement response and the input into the upper actuator. Let $H_i(\omega)$ denote this measured transfer function corresponding to location $i$, where $i=1,...,9$. If we again assume that the dowel moves as a rigid body, the slope, or rotation of the dowel can be approximated by

$$\Theta(\omega)=\frac{H_9(\omega)-H_1(\omega)}{d}, \tag{14}$$

where, again, $d$ is the total length of the dowel. The relationship between slope and displacement at location $i$ may then be estimated from

$$H_{y_i\Theta}(\omega)=\frac{H_9(\omega)-H_1(\omega)}{dH_i(\omega)}. \tag{15}$$

To compare the measured transfer function between slope and displacement at each point with the desired results, let $G_i(\omega)$ denote the ratio of the results of Eqs. (10) and (15) corresponding to location $i$,

$$G_i(\omega)=\frac{H_{y_i\Theta}(\omega)}{H_{y_m\theta_m}(\omega)}=\frac{H_9(\omega)-H_1(\omega)}{-\hat{i}kdH_i(\omega)}. \tag{16}$$

One would expect that $G_i(\omega)=1.0$ when $i$ corresponds to the middle of the dowel, $i=5$. In our case, according to Eq. (13), its magnitude would be less than 1 elsewhere.

### C. Dynamic response of the insect's body

Characterization of the dynamic response of the insect's body when driven with substrate vibration is presented in Cocroft *et al.* (2000). However, we wished to provide here an example of an additional analysis that illustrates the nature of the data provided by use of the simulator. Details of the methods are provided in that paper, but, in brief, we placed healthy individual adult female *U. crassicornis* on the dowel so that the middle leg rested at the center of the dowel (see Fig. 1). Each animal took on a natural posture as when

standing on a host plant stem. Each insect was marked with small dots of reflective paint at four locations along the midline of the body from front to back. Laser measurements were made at each point along the body. For each point, the data acquisition program first took 10 samples with the stimulus propagating in one direction, then 10 samples with the stimulus propagating in the opposite direction. The laser was then moved to the next point. A reference measurement was made on the dowel surface, near the insect's middle leg, in order to calculate the motion of the insect relative to the substrate.

## V. RESULTS

### A. Simulator performance

Figure 3 shows measurements of the magnitude and phase of $G_i(\omega)$ for the dowel shown in Fig. 1. Again, $G_i(\omega)$ is a measure of simulator performance that compares the transfer function between slope and displacement expected in an ideal beam with the transfer function between slope and displacement measured on the dowel. The signals provided to the actuators are designed to accurately create the desired relation between slope and displacement at the center of the dowel. As shown in Eq. (7), the relation between slope and displacement in an ideal traveling bending wave is independent of position. Since the dowel moves with essentially the same slope all along its length, points that are away from the center must move with greater than the ideal displacement in order to create an accurate simulation at the dowel's center, $x=d/2$. As expected, the measurements shown in Fig. 3 indicate that the quality of the simulation degrades at points further from the middle. As shown in Fig. 1, the legs of the insect occupy a region smaller than $3d/8<x<5d/8$ (dowel length between the actuators is 2.4 cm, insects legs span approximately 5 mm).

Over the region occupied by the insect, the amplitude deviation is minimal (<2 dB). The phase deviation is larger (<40 degrees), reflecting the difference between an ideal beam, in which the surface curves as bending waves propagate, and the simulator, in which the dowel surface remains essentially straight. That is, the difference between the simulator and an ideal beam reduces to a difference in slope at a given point, increasing with distance from the center and with stimulus frequency. Because the insect's leg receptors probably do not measure slope at a single point, this deviation may not be directly applicable to vibration perception. Instead, the insect must detect the slope by comparing inputs between receptors at three separate points (corresponding to the attachment points of the legs) along the surface. The situation faced by the insect is thus more clearly reflected in the following figure.

To compare the motion of the dowel with that of an ideal bending wave in the time domain, Fig. 4 shows the motion versus time relative to one period at frequencies of 500 Hz and 2500 Hz, respectively. At 500 Hz the wavelength on an actual branch is quite long relative to the size of the dowel, and thus there is very little difference in the measured and ideal bending wave curves. At 2500 Hz, however, the dowel must undergo greater motion at the ends in order for the central region to provide an adequate simulation. In each case, the motion at the center, where the insect would be located, closely approximates the ideal case. That is, the overall slope as measured between the front and back legs of an insect on the simulator is very similar to that in an ideal beam, even though the slope at a given point [see Fig. 3(b)] differs due to the curvature of the ideal beam. The measured results shown in Fig. 4 also support our assumption that the dowel remains essentially straight at the frequencies of interest.

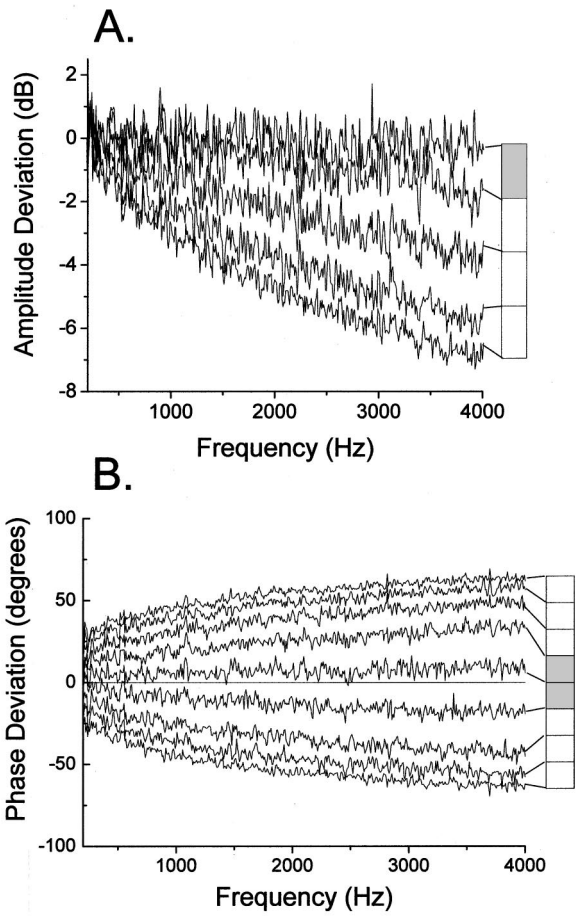


FIG. 3. Comparison of the magnitude (A) and phase (B) of the transfer function between slope and displacement measured on the dowel with that expected for an ideal bending wave [see Eq. (14)]. Note that for points away from $x=0$ (the center of the dowel), the amplitude of $G_i(\omega)$ decreases as predicted by Eq. (11). This decrease occurs because the ends of the dowel move with greater amplitude than the center. Because the slope across the dowel remains constant, the ratio of slope to displacement decreases at points away from the center. The relation between slope and displacement in the ideal bending wave is independent of position as in Eq. (5). The error in amplitude is less than 3 dB and the error in phase is less than 40 deg in the region of the dowel occupied by the insect (shaded area). In (A) only the points from the center to one end of the dowel are plotted, but the response is approximately symmetrical.

### B. Vibration of the insect

To illustrate the use of the simulator in studying directional mechanisms in insects, we complement the extensive analysis presented in Cocroft *et al.* (2000) with an example of an additional kind of analysis using data measured on an adult female *U. crassicornis*. Figure 5 shows the operating

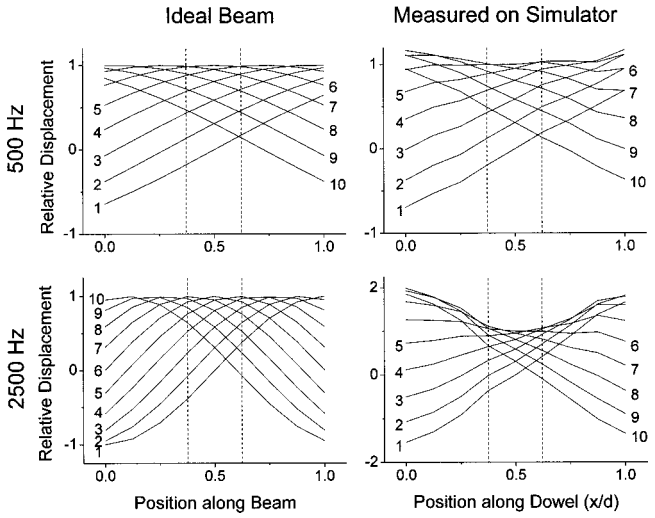


FIG. 4. Surface motion versus time during one period for an ideal beam and for the simulator. The dotted lines enclose the portion of the dowel spanned by the insect's legs. At 500 Hz the dowel length is only a fraction of a wavelength, and thus there is little difference between ideal and simulated motion. At 2500 Hz, achieving the necessary slope in the center requires greater motion of the ends of the dowel. Note the change in vertical scale for the measured results at 2500 Hz.

mode shapes measured on the insect's body for simulated bending waves traveling in opposite directions. The motion of the insect's thorax is similar to that of a rigid body on flexible legs. At lower frequencies, both ends move in phase. At higher frequencies, the back moves in the opposite direction from the front. Furthermore, the relative amplitude of motion between front and back differs depending on the direction of the stimulus. This is especially true of frequencies below 2000 Hz, which include much of the energy in the insects' communication signals (Cocroft, 1999). Note that the data were normalized with respect to motion measured on the dowel near the insect's middle leg. These data, along with those reported in Cocroft *et al.* (2000), suggest that the dynamic response of the insect's body provides a source of directional information.

## VI. DISCUSSION

In this paper we describe a simulator that reproduces the vibrational environment of an insect that communicates using plant-borne vibrations. These vibrations, which travel along stems and leaves, constitute one of the most important sources of information about the environment for insects and other arthropods (Markl, 1983; Gogala, 1985; Henry, 1994; Stewart, 1997; Barth, 1998). Furthermore, for many of the social and ecological interactions mediated by these plant-borne vibrations, localization of the vibration source is an important task (Cokl *et al.*, 1985; Pfannenstiel *et al.*, 1995). For large species (5–10 cm), arrival time delays (and perhaps amplitude differences) between an array of vibration receptors in the legs provide sufficient directional cues (Hergenroder and Barth, 1983; Latimer and Schatral, 1983; Cokl *et al.*, 1985). However, for small species (<1 cm), time and amplitude differences are much smaller, raising the question of how these species might localize a vibration source. The

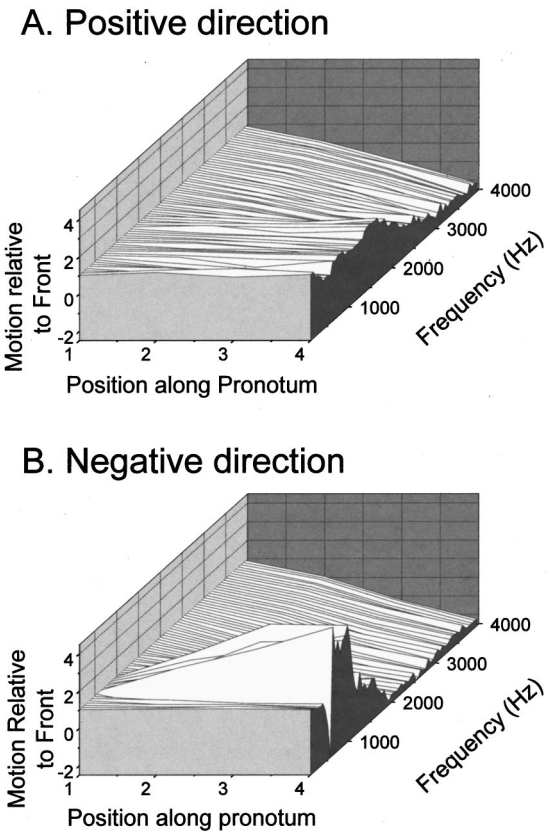


FIG. 5. An example from one insect of the effect of direction of substrate vibrations on the dynamic response of the body (for full results see Cocroft *et al.*, 2000). The measured motion is shown versus frequency, measured on the insect for simulated waves traveling in positive and negative directions. In each case the insect's motion is similar to a rigid body on flexible legs. At lower frequencies, both ends of the insect move in phase. At higher frequencies (>2500 Hz), the back moves in the opposite direction from the front. For waves traveling in the negative direction, the back of the insect moves with significantly greater amplitude than the front. The frequency dependence of the operating mode shapes is strongly influenced by the direction of propagation.

simulator described here is a useful tool that facilitates the investigation of directional sensing in small arthropods.

The simulator closely approximates the relationship between slope and displacement characteristic of bending waves propagating along an ideal beam. Because the dowel is straight, it cannot reproduce bending wave motion along its entire length, but only in a region in the center of the dowel. The width of this region varies with the wavelength of the stimulus: in order to create the required surface motion in the center, the ends must be moved through a greater and greater excursion as frequency increases. For our study species, the treehopper *U. crassicornis*, the biologically relevant frequency range appears to be mostly under 4 kHz (Cocroft, 1999). For this frequency range, the region of the simulator occupied by an insect (legs spanning 5 mm at the center of the dowel) closely approximates the vibrational environment created by propagating bending waves. The simulator allowed us to investigate the influence of stimulus direction on the dynamic response of an insect's body to substrate vibration. Detailed results presented in Cocroft *et al.* (2000) reveal a marked mechanical directionality in the motion of the insects body relative to the substrate. In this report we pro-

vided an additional type of analysis, also revealing an effect of direction on the motion measured across the insect's body. The dynamic response of the body to vibration of the substrate converts the small time differences between the arrival of the stimulus at the front and back legs (55 $\mu$s at 500 Hz) into a relatively large amplitude difference across the body (about 10 dB at some frequencies). This difference may arise from the interaction of the two modes of vibration (rotational and translational) detected in the motion of the body (see Gerzon, 1994). Because motion at the front and back of the body differs depending on stimulus direction, it provides robust directional cues that could in principle be detected by the nervous system (this has not yet been investigated; see discussion in Cocroft *et al.*, 2000). These results raise the possibility of a new means of directional sensing in insect vibrational perception.

In the case of our study species, the performance of the simulator most closely approximated bending waves across a small area in the center of the dowel spanned by the insect's legs, and for lower frequencies that contain most of the energy in the species' own signals. Use of this simulator design for other species is warranted if their dimensions, and the frequencies used, fall within a similar range. For larger insects, Eq. (11) can be used to assess whether this apparatus is appropriate (or, alternatively, to estimate the dimensions of a suitable apparatus).

This experimental apparatus should facilitate investigation of other questions involving vibration perception in insects. For example, the creation of steady-state bending wave motion should facilitate investigation of the neural coding of the directional information present in the dynamic response of the body. Furthermore, use of natural time signals that evoke an orienting response (such as those used in mate location; e.g., Cokl *et al.*, 1999) will allow behavioral assays of directional ability and of the signal features essential for directional sensing.

## VII. SUMMARY

We describe a bending-wave simulator capable of reproducing the vibrational environment of many small insects and other arthropods that use plant-borne vibrations in social and ecological interactions. The purpose of this simulator is to facilitate the study of directional sensing mechanisms, because it can mimic bending waves propagating in opposite directions along a stem, thus delivering stimuli that are identical in all features except for direction of propagation. This task is difficult using natural substrates.

The simulator consists of a short section of dowel driven by two actuators. In the case of bending waves propagating along an ideal beam, the relationship between slope and displacement is independent of position along the beam. This requires curvature of the stem. In contrast, the dowel segment remains essentially straight (i.e., the slope is constant across the dowel). As a result, exact reproduction of the relationship of slope and displacement characteristic of bending waves is possible only at the center of the dowel. The simulator departs from this relationship toward the ends of the dowel, because the ends must be moved with a greater amplitude in order to achieve the necessary slope in the middle.

For a small insect positioned at the center of the dowel, and using the relatively low frequency range of biologically relevant signals, the simulator provides a close approximation of propagating bending waves. Measurements of the dynamic response of the body of a tree-hopper (*Umbonia crassicornis*) reveal a mechanical directionality that may provide a means of vibration localization.


## ACKNOWLEDGMENTS

R.N.M., R.B.C., and C.B. were supported by NIDCD Grant No. 1R01DC03926-01. R.N.M., C.B., and D.B. were also supported by NSF Grant No. BCS9315854. Support for R.B.C. was also provided by the Olin Foundation. We thank D. Kunkel for Fig. 1.


## APPENDIX: CONSTRUCTION OF THE EXCITATION SIGNALS

In the following, we describe the procedure for creating the signals input into the actuators on each end of the dowel shown in Fig. 1. The approach is an extension of that originally due to Rice (1954) and adapted by Shinozuka (1972) and Miles (1992).

Given the power spectral density for a complex system one can construct a time series that will have the desired power spectrum. If $S_{y_1y_1}(\omega)$ is the double sided power spectrum of the desired signal, $y_1(t)$, the $y_1(t)$ may be approximated by

$$y_1(t)=2\sum_{n=0}^{N-1}[S_{y_1y_1}(\omega_n)\Delta\omega]^{1/2}\cos(\omega_n t-\phi_n), \qquad \text{(A1)}$$

where $\phi_n$ are uniformly distributed random numbers on the interval from 0 to $2\pi$ and

$$\omega_n=n\Delta\omega, \qquad \text{(A2)}$$

with

$$\Delta\omega=\omega_{\max}/N, \qquad \text{(A3)}$$

where $\omega_{\max}$ is the maximum frequency in the power spectrum $S_{y_1y_1}(\omega)$, and $N$ is the total number of terms in the summation in Eq. (A1).

Equation (A1) simulates the time series as a distribution of sinusoidal signals having random phases. Unfortunately, this expression requires the computation of a large number of cosine functions at each desired value of the time, *t*. A considerable improvement in computational efficiency can be obtained by recasting Eq. (A1) to allow the use of the fast-Fourier transform. To accomplish this, note that Eq. (A1) may be written as

$$y_1(t)=2\,\mathrm{Re}\left[\sum_{n=0}^{N-1}[S_{y_1y_1}(\omega_n)\Delta\omega]^{1/2}e^{\hat{\imath}\omega_n t}e^{-\hat{\imath}\phi_n}\right], \qquad \text{(A4)}$$

where Re[·] denotes the real part and, as before, $\hat{\imath}$ is $\sqrt{-1}$.

If the simulated time series, $y_1(t)$ is needed only at discrete values of time, *t*, then let

$$y_j=y_1(t_j)=y_1(j\Delta t), \qquad \text{(A5)}$$

where the time duration between the equally spaced sample times is $\Delta t$. Evaluating Eq. (A4) at $t=t_j$ gives

$$y_1(j\Delta t)=2\,\mathrm{Re}\left[\sum_{n=0}^{N-1}[S_{y_1y_1}(\omega_n)\Delta\omega]^{1/2}e^{\hat{\imath}\omega_n j\Delta t}e^{-\hat{\imath}\phi_n}\right]. \tag{A6}$$

To satisfy the Nyquist sampling criterion, the time series, $y_1(t)$ must be sampled at a high enough rate to obtain two samples during one period of the highest frequency component in the original input power spectrum, $S_{y_1y_1}(\omega)$. This gives

$$\Delta t=\frac{2\pi}{\omega_{\max}}\frac{1}{2}. \tag{A7}$$

Substituting Eqs. (A3) and (A7) into Eq. (A6) gives

$$y_1(j\Delta t)=2\,\mathrm{Re}\left[\sum_{n=0}^{N-1}[S_{y_1y_1}(\omega_n)\Delta\omega]^{1/2}e^{-\hat{\imath}\phi_n}e^{\hat{\imath}nj2\pi/2N}\right]. \tag{A8}$$

Equation (A8) may be evaluated using a fast-Fourier transform (FFT) algorithm by noting that given a discrete sequence, $a_n$, the FFT provides an efficient means of computing $A_j$, where

$$A_j=\sum_{n=0}^{N-1}a_n e^{-\hat{\imath}2\pi jn/N},\qquad \text{for } j=0,1,2,...,N-1. \tag{A9}$$

Equation (A8) may be evaluated using a FFT by defining a sequence,

$$\begin{aligned}a_n&=2[S_{y_1y_1}(\omega_n)\Delta\omega]^{1/2}e^{-\hat{\imath}\phi_n},\quad \text{for } n\leqslant N-1\\&=0,\quad \text{for } n\leqslant N.\end{aligned} \tag{A10}$$

Equation (A8) may then be written as

$$y_{1_j}=\mathrm{Re}\left[\sum_{n=0}^{2N-1}a_n e^{\hat{\imath}nj2\pi/2N}\right],\quad \text{for } j=0,1,2,...,2N-1, \tag{A11}$$

where $y_{1_j}=y_1(j\Delta t)$. Because we are taking the real part of the result of the summation, taking the complex conjugate of the right-hand side of Eq. (A11) gives

$$y_{1_j}=\mathrm{Re}\left[\sum_{n=0}^{2N-1}a_n e^{-\hat{\imath}nj2\pi/2N}\right],\quad \text{for } j=0,1,2,...,2N-1. \tag{A12}$$

This is equivalent to

$$y_{1_j}=\mathrm{Re}[\mathrm{FFT}(a_n)], \tag{A13}$$

where FFT$[\cdot]$ denotes the fast-Fourier transform. Note that the length of the sequence, $a_n$ is $2N$.

The construction of another time series, $y_2(t)$ which is related to $y_1(t)$ according to the transfer function in Eq. (7) may be accomplished by defining a sequence that is analogous to Eq. (A10),

$$\begin{aligned}b_n&=2[S_{y_1y_1}(\omega_n)\Delta\omega]^{1/2}e^{-\hat{\imath}\phi_n}H_{y_1y_2}(\omega_n),\quad \text{for } n\leqslant N-1\\&=0,\quad \text{for } n\geqslant N,\end{aligned} \tag{A14}$$

where the transfer function $H_{y_1y_2}(\omega_n)$ is computed as in Eq. (7),

$$H_{y_1y_2}(\omega_n)=\frac{1-\hat{\imath}k_nd/2}{1+\hat{\imath}k_nd/2} \tag{A15}$$

and

$$k_n=\frac{\omega_n}{c}=\frac{2\pi f_n}{c_c\sqrt{f_n}}=2\pi\sqrt{f_n}/c_c, \tag{A16}$$

with $\omega_n=2\pi f_n$. The time series is then computed from

$$y_{2_j}=\mathrm{Re}[\mathrm{FFT}(b_n)], \tag{A17}$$

with $y_2(j\Delta t)=y_{2_j}$ for $j=0,1,2,...,2N-1$.


Aicher, B., and Tautz, J. (**1990**). ''Vibrational communication in the fiddler crab *Uca pugilator*. I. Signal transmission through the substratum,'' J. Comp. Physiol. **166**, 345–353.

Barth, F. G. (**1993**). ''Sensory guidance in spider pre-copulatory behaviour,'' Comp. Biochem. Physiol. **104A**, 717–733.

Barth, F. G. (**1998**). ''The vibrational sense of spiders,'' in *Comparative Hearing: Insects*, edited by R. R. Hoy, A. N. Popper, and R. R. Fay, Springer Handbook of Auditory Research, series edited by R. R. Fay and A. N. Popper (Springer, New York), pp. 228–278.

Brownell, P. H. (**1977**). ''Compressional and surface waves in sand: used by desert scorpions to locate prey,'' Science **197**, 479–482.

Brownell, P. H., and Farley, R. D. (**1979**). ''Orientation to vibrations in sand by the nocturnal scorpion *Paruroctonus mesaensis*: mechanism of target localization,'' J. Comp. Physiol. **131**, 31–38.

Cocroft, R. B. (**1996**). ''Insect vibrational defence signals,'' Nature (London) **382**, 679–680.

Cocroft, R. B. (**1999**). ''Offspring-parent communication in a subsocial treehopper (Hemiptera: Membracidae: *Umbonia crassicornis*),'' Behaviour **136**, 1–21.

Cocroft, R. B., Tieu, T., Hoy, R. R., and Miles, R. N. (**2000**). ''Directionality in the mechanical response to substrate vibration in a treehopper (Hemiptera: Membracidae: *Umbonia crassicornis*),'' J. Comp. Physiol. B **186**, 695–705.

Cokl, A., Otto, C., and Kalmring, K. (**1985**). ''The processing of directional vibratory signals in the ventral nerve cord of *Locusta migratoria*,'' J. Comp. Physiol. A **156**, 45–52.

Cokl, A., Virant-Doberlet, M., and McDowell, A. (**1999**). ''Vibrational directionality in the southern green stink bug, *Nezara viridula* (L.), is mediated by female song.'' Anim. Behav. **58**, 1277–1283.

Cremer, L., and Heckl, M. (**1988**). *Structure-Borne Sound. Structural Vibrations and Sound Radiation at Audio Frequencies* (Springer, Berlin), 2nd ed.

Gerzon, M. A. (**1994**). ''Applications of Blumlein shuffling to stereo microphone techniques,'' J. Audio Eng. Soc. **42**, 435–453.

Gogala, M. (**1985**). ''Vibrational communication in insects (biophysical and behavioural aspects),'' in *Acoustic and Vibrational Communication in Insects*, edited by K. Kalmring and N. Elsner (Verlag Paul Parey, Berlin), pp. 117–126.

Henry, C. S. (**1994**). ''Singing and cryptic speciation in insects,'' Trends Ecol. Evol. **9**, 388–392.

Hergenroder, R., and Barth, F. G. (**1983**). ''Vibratory signals and spider behavior: how do the sensory inputs from the eight legs interact in orientation?,'' J. Comp. Physiol. **152**, 361–371.

Kalmring, K. (**1985**). ''Vibrational communication in insects (reception and integration of vibratory information),'' in *Acoustic and Vibrational Communication in Insects*, edited by K. Kalmring and N. Elsner (Verlag Paul Parey, Berlin).

Keuper, A., and Kuhne, R. (**1983**). ''The acoustic behaviour of the bushcricket *Tettigonia cantans*. II. Transmission of airborne-sound and vibration signals in the biotope,'' Behav. Processes **8**, 125–145.

Latimer, W., and Schatral, A. (**1983**). ''The acoustic behaviour of the bushcricket *Tettigonia cantans*. I. Behavioural responses to sound and vibration,'' Behav. Processes **8**, 113–124.

Markl, H. (**1983**). ''Vibrational communication,'' in *Neurobiology and Behavioral Physiology*, edited by F. Huber and H. Markl (Springer-Verlag, Berlin), pp. 332–353.
Michelsen, A., Fink, F., Gogala, M., and Traue, D. (**1982**). ''Plants as transmission channels for insect vibrational songs,'' Behav. Ecol. Sociobiol. **11**, 269–281.
Miles, R. N. (**1992**). ''Effect of spectral shape on acoustic fatigue life estimates.'' J. Sound Vib. **153**, 376–386.
Miles, R. N., Robert, D., and Hoy, R. R. (**1995**). ''Mechanically coupled ears for directional hearing in the parasitoid fly *O. ochracea*,'' J. Acoust. Soc. Am. **98**, 2059–2070.
Pfannenstiel, R. S., Hunt, R. E., and Yeargan, K. V. (**1995**). ''Orientation of a hemipteran predator to vibrations produced by feeding caterpillars,'' J. Insect Behav. **8**, 1–9.
Rice S. O. (**1954**). *Selected Papers on Noise and Stochastic Processes*, edited by N. Wax (Dover, New York).
Shinozuka, M. (**1972**). ''Monte Carlo solution of structural dynamics,'' Comput. Struct. **2**, 855–874.
Stewart, K. W. (**1997**). ''Vibrational communication in insects: epitome in the language of stoneflies?,'' Am. Entomol. **1997**, 81–91.
Wood, T. K. (**1983**). ''Brooding and aggregating behavior of the treehopper, *Umbonia crassicornis*,'' Natl. Geogr. Soc. Res. Rep. **15**, 753–758.